

PAPER

Mosquitoes modulate leg dynamics at takeoff to accommodate surface roughness

To cite this article: Nicholas M Smith *et al* 2019 *Bioinspir. Biomim.* **14** 016007

View the [article online](#) for updates and enhancements.



IOP | ebooksTM

Bringing you innovative digital publishing with leading voices
to create your essential collection of books in STEM research.

Start exploring the collection - download the first chapter of
every title for free.

Bioinspiration & Biomimetics



PAPER

RECEIVED
27 July 2018

REVISED
26 October 2018

ACCEPTED FOR PUBLICATION
1 November 2018

PUBLISHED
27 November 2018

Mosquitoes modulate leg dynamics at takeoff to accommodate surface roughness

Nicholas M Smith¹, Grace V Clayton, Hiba A Khan and Andrew K Dickerson¹

Department of Mechanical and Aerospace Engineering, University of Central Florida, Orlando, FL, 32816, United States of America

¹ Author to whom any correspondence should be addressed.

E-mail: dickerson@ucf.edu

Keywords: leg force, leg power, traction, takeoff kinematics, takeoff kinetics

Supplementary material for this article is available [online](#)

Abstract

Insects perform takeoffs from a nearly unquantifiable number of surface permutations and many use their legs to initiate upward movement prior to the onset of wingbeats, including the mosquito. In this study we examine the unprovoked pre-takeoff mechanics of *Aedes aegypti* mosquitoes from two surfaces of contrasting roughness, one with roughness similar to polished glass and the other comparable to the human forearm. Using high-speed videography, we find mosquitos exhibit two distinct leg actions prior to takeoff, the widely observed push and a previously undocumented leg-strike, where one of the rearmost legs is raised and strikes the ground. Across 106 takeoff sequences we observe a greater incidence of leg-strokes from the smoother surface, and rationalize this observation by comparing the characteristic size of surface features on the mosquito tarsi and each test surface. Measurements of pre-takeoff kinematics reveal both strategies remain under the mechanosensory detection threshold of mammalian hair and produce nearly identical vertical body velocities. Lastly, we develop a model that explicates the measured leg velocity of striking legs utilized by mosquitoes, 0.59 m s^{-1} .

1. Introduction

Traditional studies of insect takeoff kinematics have focused on insect morphology [1–5] and takeoff stimulus [6, 7] without consideration of the role of surface conditions on takeoff mechanics. In nature, insects launch from a vast variety of surfaces offering variation in roughness and surface obstacles with which legs and wings must contend. As technology allows for the miniaturization of robotic flyers, predicted to resolve many surveillance, reconnaissance, and exploratory challenges [8, 9], takeoff conditions and takeoff surface topography pose a greater impact on flyer performance. Small insects provide kinematic templates for successful launching from a vast array of surfaces. In this study, we compare the takeoffs of *Aedes* (*Ae.*) *aegypti* mosquitoes, vector of the Zika and yellow fever viruses [10], from a surface the smoothness of glass to a surface the roughness of human skin. Understanding how insects respond to various environmental challenges [11–18], including complex surfaces will inform the areas of small unmanned aerial systems (sUAS) development and vector control.

Insect takeoff is both scenario and species dependent, as we discuss herein. Furthermore insect takeoff may be further delineated into two categories, jumping and non-jumping, where one utilizes leg contributions and the other relies predominantly on wing flapping lift. Mosquitoes are known [6] to employ a two-step takeoff that is initiated with the legs prior to wing engagement, a shared behavior across scale and species. Locust takeoffs are described by a ‘jump’ prior to the first wingbeat, lasting 33 ms, whereby leg and wing actions are not overlapping [5]. In contrast, droneflies utilize wing and leg thrust in synchrony, gradually increasing stroke amplitude, beginning 10 ms after takeoff initiation, whilst monotonically decreasing leg output force through the twelfth wingbeat [2]. Droneflies exchange speed for a relatively smooth takeoff, leaving the ground in 40 ms. Other insects choose speed over stability when startled [19]. Common fruit flies perform two distinct takeoff strategies, one voluntary and the other responsive [7]. Butterflies, which have a cord-span ratio >1 , utilize a ‘fling’ method which pitches the thorax through large angles during low frequency wing strokes [3], and although

their wing to body ratio is relatively large, they utilize leg forces at takeoff to increase upward acceleration [20]. Damselflies employing voluntary non-jumping takeoffs are able to generate $3\times$ their body weight in the first half wingbeat of takeoff and utilize forewing-hindwing interactions to enhance lift [1].

Parasitic flyers, such as mosquitoes, often require their flight operations be clandestine to avoid detection by large hosts, thereby placing restrictions on forces transmitted to the takeoff surface. The threshold of mechanosensory detection of forces by the nerves surrounding human hair is 0.07 mN [21], which is widely accepted to be the lightest touch we can detect. In response, mosquitoes have adapted ‘light-footed’ takeoff sequencing, which varies with weight as they feed [6]. A blood-fed *Anopheles coluzzi* mosquito weighs approximately $3\times$ its unfed bodyweight and adjusts its takeoff by utilizing more wing-based lift and correspondingly slow extension of legs, resulting in a maximum surface reaction force of 0.02 mN over a total takeoff time [6] of 26.3 ms. Despite the extensive documentation of insect takeoff and external influences, missing from literature is a study that incorporates the affect of surface characteristics on the adaptive takeoff sequence of flyers with multiphase takeoffs, such as mosquitoes.

In this combined theoretical and experimental study, we investigate the takeoffs, as seen in figure 1(a), of *Ae. aegypti* mosquitoes from surfaces of contrasting roughness. In section 2, we begin with our experimental methods for creating test surfaces and filming takeoffs. In section 3, we present the observed takeoff kinematics and associated substrate forces. We rationalize takeoff techniques by comparing surface features with those found on the mosquito tarsi, and discuss the implications of our study and avenues for future research in section 4. We provide conclusions from our work in section 5.

2. Experimental methods

2.1. Takeoff experiments

Takeoffs were filmed using Photron AX-100 and UX-100 high-speed cameras at 1000–4000 fps and 1/8000s shutter speed. The glass mosquito flight arena is shown in figure 2 and measures $76 \times 79 \times 152$ mm. A 7.5 mm ID glass tube is inserted 100 mm above the arena floor through which mosquitoes walk to enter the arena, emerging on a horizontal takeoff platform measuring 210 mm². Mosquitoes are transported with an aspirator to a larger diameter holding area at end of the tube (not pictured), allowing mosquitoes to exit toward the arena under their own volition. The tube dwell times ranged from 1–15 min. Mosquitoes preferred to exit the holding area when the capacity exceeded 15 mosquitoes. No anesthesia was used prior to takeoff experiments. Following experiments, mosquitoes were anesthetized with carbon dioxide for removal from the flight arena. Individuals were euthanized following trials to avoid pseudoreplication.

2.2. Surface characterization

Surface A is an unmodified, polished acrylic sheet. Surface B is made by roughening polished acrylic with a 12.7 cm (5 inch) orbital hand sander using 220 grit sandpaper. Surface roughnesses is measured using a KLA-Tencor Alpha-Step 500 profilometer in two dimensions to ensure surface homogeneity. Scanning electron microscope (SEM) images were garnered with a Phenom G1 desktop SEM.

2.3. Mosquito mass measurements

Mass measurements were performed using a Sartorius Secrúa 225D-1s microbalance using 30 anesthetized and fully-intact mosquitoes. Simultaneous mass measurement of 30 mosquitoes reduces the influence of instrument error. Leg mass is done by gender in a similar manner by anesthetizing a group of mosquitoes and extracting 20 rearmost legs, those used for the leg-strike takeoffs. The center of mass of the leg was determined digitally using imageJ and by assuming the density of leg tissue is uniform throughout. A binary image used to estimate a leg’s center of mass and produced from figure 1(b) is provided in figure S1 (stacks.iop.org/BB/14/016007/mmedia).

3. Results

We film 106 horizontal takeoffs of non-blood fed, male and female, *Ae. aegypti* mosquitoes at 1000–4000 fps in a custom flight arena in which mosquitoes emerge from a tube onto a platform of varying surface roughness (see section 2). Restriction of the tube diameter prevents flight inception within the tube, mandating mosquitoes launch from the horizontal platform. Using this method, no anesthetization was used to place mosquitoes onto the takeoff platform. Under voluntary takeoff conditions, we observe *Ae. aegypti* mosquitoes employ two distinct takeoff strategies. The first, dubbed a ‘push’, is described by the quick extension of legs to their maximum extent. Most commonly, all six legs participate in pushing but we occasionally observe a 4- or 5-legged push. Legs consist of three sections, the femur, tibia, and tarsus, as shown in figure 1(b). During takeoff, only the tarsi contact the ground. As the mosquito body moves upward, the tarsi slide inward, frequently meeting before lifting off. The second strategy, a ‘leg-strike’, is initiated by the downward swing of one elevated hind leg. The transfer of momentum from the subsequent strike against the substrate initiates body lift. Following the leg-strike, a six-legged push commences, comparable to a purely pushing takeoff. Below we compare the performance and substrate forces for both takeoff types.

3.1. Pushes

Mosquitoes begin a pushing takeoff with their legs planted on the takeoff platform. In unison, the legs straighten and draw inward, pushing the mosquito’s body upward as wingbeats commence. This sequence of leg extension and body lift is displayed pictorially

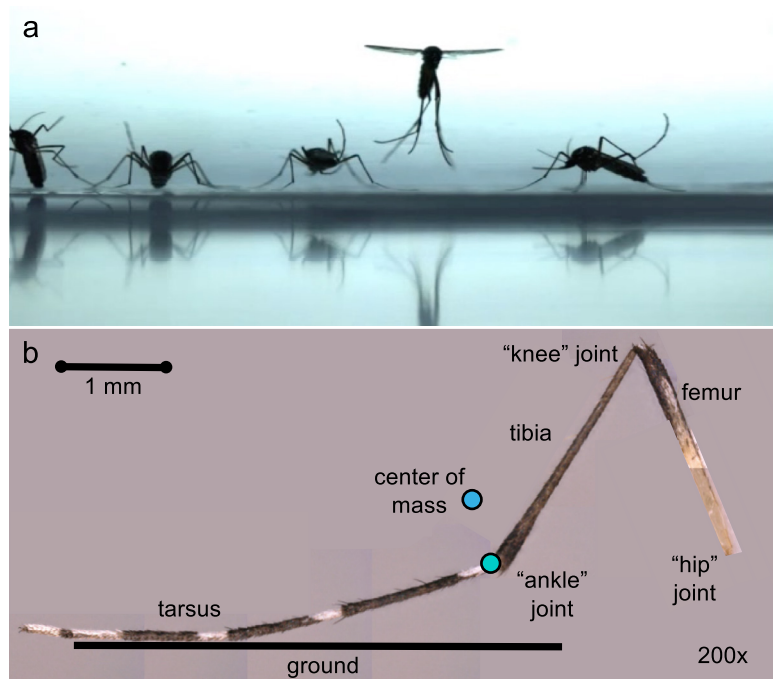


Figure 1. Image of (a) multiple mosquitoes sitting at base platform with one mid-action takeoff and (b) a composite image of a mosquito's striking leg at 200 \times .

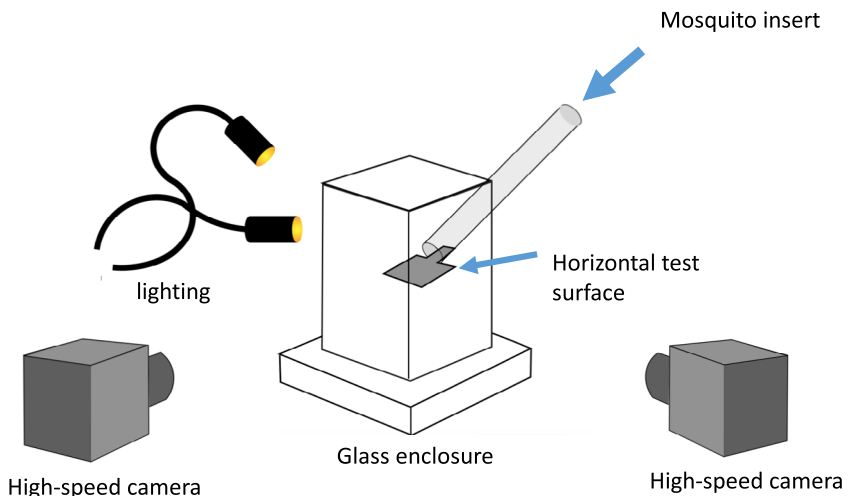


Figure 2. Image of mosquito flight arena experimental setup.

in figure 3 and shown in Movie S1. In the following calculations of force and power, we consider only the dynamics of female mosquitoes. The legs experience rapid extension during pushing, beginning with a contracted angle of $88.5 \pm 16.9^\circ$, $N = 5$, and extending to $120.2 \pm 20.5^\circ$, $N = 5$, over the course of time preceding the first wingbeat $\tau_w = 5.5 \pm 2.2$ ms, $N = 10$, and corresponding to the leftmost region of figure 3. The resulting angular velocity, 16 rev s $^{-1}$, is sufficient to produce a lift velocity of $U = 0.38 \pm 0.17$ m s $^{-1}$, $N = 10$, generating an upward acceleration equivalent to seven gravities (g).

We assume that each leg contributes equally to liftoff in our analysis. We likewise assume that push-

ing forces are greatest before wingbeats begin, since the aerodynamic lift force created by the wings is $\sim 1\text{--}5$ times greater than that of the legs [6], and so we only consider the short moments prior to the first full wingbeat τ_w in our analysis of applied substrate forces. The total time to tarsal liftoff $\tau_{lift} = 11.6 \pm 1.6$ ms, $N = 10$. Finally, we assume the force provided by the legs remains constant throughout τ_w and that tarsi do not slip outwardly, as done in previous studies [22–25]. We discuss the implications of this assumption and provide an alternative in section 4. Conservation of momentum and impulse yields

$$F_p = \frac{m}{6} \left(\frac{U}{\tau_w} + g \right), \quad (1)$$

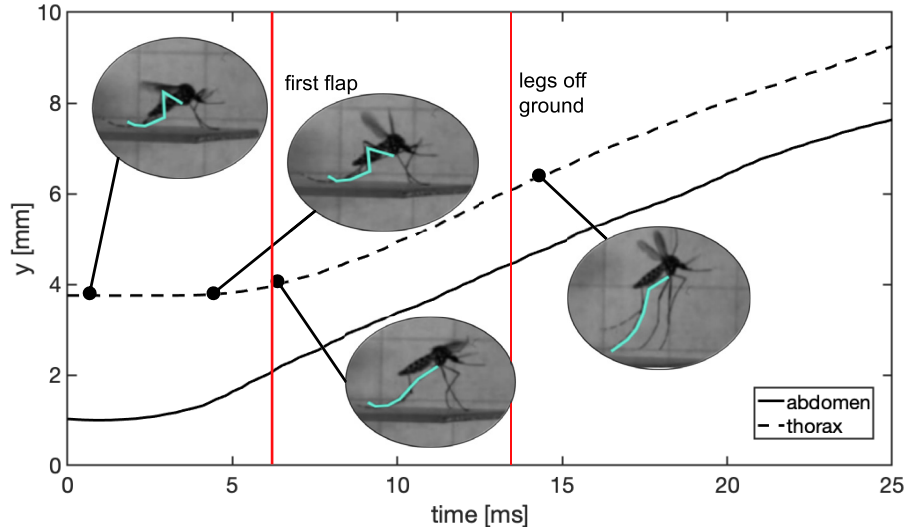


Figure 3. Steps defined for a push takeoff overlaid onto a elevation versus time plot for abdomen and thorax positions.

where $F_P = 0.027 \text{ mN}$ is the normal pushing force per leg exerted on the takeoff platform, $m = 2.06 \text{ mg}$ is the mosquito's body mass, averaged over 30 individual females, and $g = 9.81 \text{ m s}^{-2}$ is the acceleration due to gravity. We note this value is well below the cutaneous neuron mechanosensory threshold of human hair [21], 0.07 mN, but greater than those previously measured for *Anopheles coluzzi* [6]. The average power generated by a pushing leg during takeoff is given by

$$P_P = \frac{mU}{6} \left(\frac{U}{2\tau_w} + g \right), \quad (2)$$

where $P_P = 5.78 \mu\text{W}$.

3.2. Leg-strikes

Leg-strike takeoffs are modifications to pushing takeoffs, and are of similar duration to purely pushing takeoffs at $\tau_w = 9.6 \pm 1.6 \text{ ms}$, $N = 10$, and $\tau_{\text{lift}} = 13.1 \pm 2.3 \text{ ms}$, $N = 10$. Achieving nearly identical vertical body velocity at first wingbeat, $U = 0.35 \pm 0.17 \text{ m s}^{-1}$, $N = 10$. The takeoff begins as an elevated rear leg swings rapidly downward and strikes the takeoff substrate at $U_{\text{leg}} = 0.59 \pm 0.06 \text{ m s}^{-1}$, $N = 25$, measured by tracking the 'ankle joint' of the leg as denoted in figure 1(b). The tracked position on the leg is a surrogate for the leg's center of mass, which is nearby and likewise denoted in figure 1(b). The downward swing of the leg is pictured in figure 4 and shown in Movie S2. Through video analysis at 10 000 fps we measure leg swing distance $d_s = 1.8 \pm 0.4 \text{ mm}$, $N = 3$, and impact time $\tau_i = 0.8 \pm 0.10 \text{ ms}$, $N = 3$. Following impact of the swing, all legs push upward, and generating a comparable ground reaction force. The force of the striking leg F_{LS} = 0.025 mN and is given by

$$F_{\text{LS}} = \frac{m_{\text{leg}} U_{\text{leg}}}{\tau_i}, \quad (3)$$

where the mass of the striking leg $m_{\text{leg}} = 33.5 \mu\text{g}$. Like F_P , F_{LS} lies well below the mechanosensory threshold in humans [21], and thus a striking leg is imperceptible to a human host. The average power required to achieve U_{leg} is

$$P_{\text{LS}} = \frac{m_{\text{leg}} U_{\text{leg}}^2}{2\tau_s}, \quad (4)$$

where the swing time from first movement until first contact with the ground is represented as

$$\tau_s = \frac{d_s}{\chi U_{\text{leg}}}, \quad (5)$$

and experimentally measured $\chi = 0.71$ compensates for the ramp in leg speed up from zero to U_{leg} . The resulting power given to the single striking leg $P_{\text{LS}} = 1.36 \mu\text{W}$ is considerably less than the power required of a pushing leg according to equation (2), $P_P = 5.78 \mu\text{W}$.

A leg's center of mass striking the ground a perpendicular distance $\ell = 2.58 \pm 0.14 \text{ mm}$ from the body's center of mass has consequences on body pitch and lift. If we estimate the center of mass to lie midway between the aft of the abdomen and the base of the proboscis, we may calculate the pitch of the body during the strike by first finding the angular acceleration $\alpha = (F_{\text{LS}}/\bar{I})\ell = 18.7 \times 10^3 \text{ rad s}^{-2}$ imparted to the body during the leg's impact time, for a cylindrical mosquito of length $L = 4.48 \pm 0.34 \text{ mm}$. The mass moment of inertia for a cylinder rotating longitudinally about its center is $\bar{I} = mL^2/12$. The corresponding change in body angle during the ephemeral impact time τ_i is a minuscule 0.34° . Such a small rotation is not perceptible in tracking data. We calculate the impulsive force the striking leg generates, an upward body velocity of 0.01 m s^{-1} , which is 3% the body velocity at first wingbeat. It may appear the leg-strike is of little consequence, but the result is unloaded

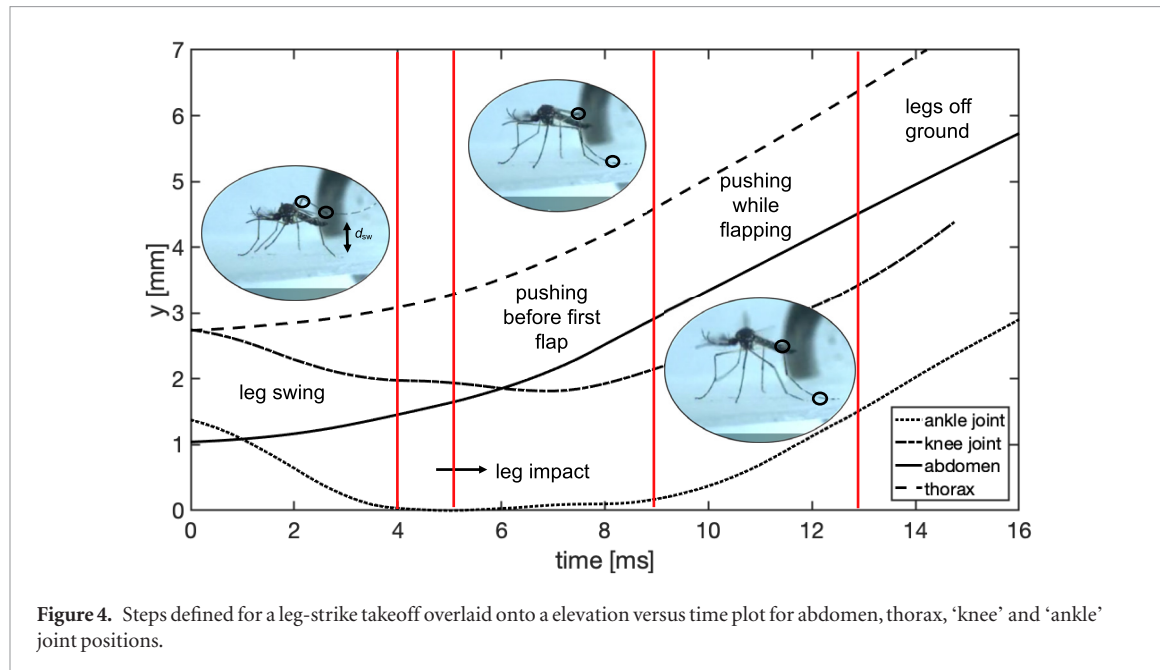


Figure 4. Steps defined for a leg-strike takeoff overlaid onto a elevation versus time plot for abdomen, thorax, ‘knee’ and ‘ankle’ joint positions.

tarsi at the onset of the pushing phase, which is likely to retard tarsal engagement of the surface when pushing commences, allowing for increased traction.

3.3. Surface roughness drives takeoff strategy

The two surfaces used in this study are pictured in figures 5(a) and (b), alongside an *Ae. aegypti* tarsus at the same scale. Surface A (figure 5(a)) is polished acrylic, having an arithmetic mean deviation roughness $R_q = 3.1 \text{ nm}$, the approximate roughness of glass [26]. Surface B (figure 5(b)) is acrylic roughened with sandpaper, and has $R_q = 43 \mu\text{m}$, approximately the roughness of human skin [27]. The mosquito tarsus (figure 5(c)) is covered in feathery scales which aid in standing on a water surface [28], roughly 10–15 μm in size according to our measurements.

Takeoff strategy is driven by surface roughness. As seen in figure 5(d), polished Surface A resulted in leg-strokes (66%) dominating pushes (34%), $N = 44$, when considering both male and female mosquitoes. Surface B, the rougher of the two, evokes greater frequency of pushing (56%) and leg-strokes (44%) in minority, $N = 62$. We find takeoffs from these two surfaces to be statistically different when performing a Fisher’s exact test for contingency, with $p = 0.0301$. However, no such strategy preference exists based on gender for either surface Surface A ($p = 0.5350$) or Surface B ($p = 0.5792$).

We rationalize the shift in strategy preference by observations of purely pushing takeoff on polished and roughened surfaces. When pushing from roughened Surface B, mosquitoes tarsi remain in place through the bulk of leg extension and draw inward as legs reach their maximum extent (figure 3). The alignment of the feathery structures on the tarsi likely provide anisotropic friction and aid this maneuver. As seen in figure 5(c), the features on the tarsus match the scale of the disparities on Surface B, but are larger than

the disparities of Surface A. In contrast to Surface B, pushing from Surface A may result in the outward slip of the tarsi (Movie S3), thereby reducing the efficacy of the push. Traction on Surface A is so little, we observe some mosquitoes rest their abdomen on the takeoff platform prior to takeoff due to the severe splaying of their legs.

3.4. Model for optimal leg-strike takeoff

Mosquitoes may exercise a range of leg-striking speeds to initiate takeoff, as would any flyer employing this method of launch. However, choice of leg-striking speed will influence takeoff dynamics in both leg-strike and push phases of takeoff. A mosquito launching from a host should do so quickly with sufficient velocity to escape the surface and do so undetected. Therefore, we surmise mosquitoes instinctively keep total takeoff time consistent while minimizing force exerted on the host. We rationalize the observed leg impact speed U_{leg} by modeling each portion of takeoff, swing, impact, and push, while fixing time to first flap τ_w , takeoff speed U , leg swing distance d_s , and leg impact time τ_i to the average observed in experiments and provided in table 1.

As a result of the leg striking the ground, the body is pushed upward at

$$U_0 = U_{\text{leg}} m_{\text{leg}} / m. \quad (6)$$

The time remaining for the pushing phase is $\tau_w - \tau_s - \tau_i$, over which the six pushing legs need to generate an additional upward body velocity of $U - U_0$. Combining equations (1), (3), (5) and (6), we develop a model by which we can vary U_{leg} and generate F_{LS} , and the pushing force per leg in the portion of takeoff following leg impact,

$$F_{\text{P,LS}} = \frac{m}{6} \left(\frac{U - U_0}{\tau_w - \tau_s - \tau_i} + g \right). \quad (7)$$

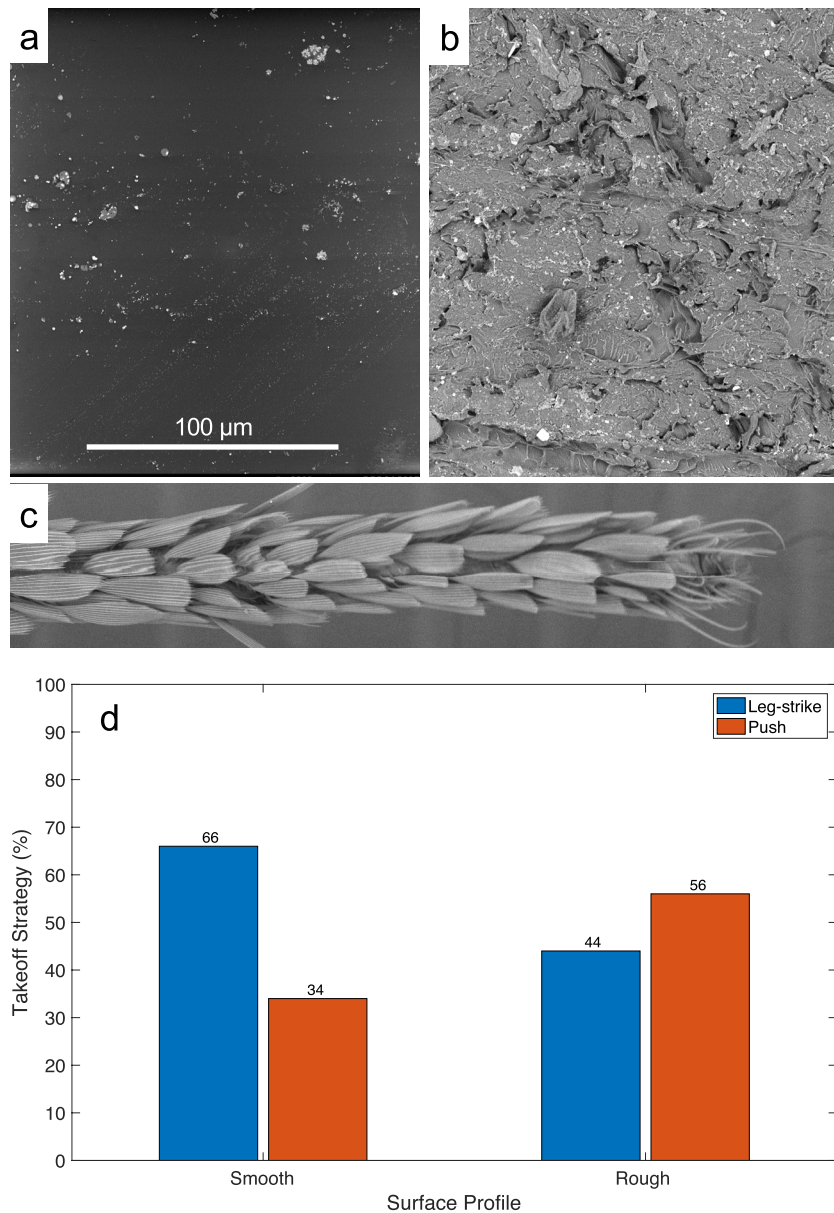


Figure 5. SEM images of (a) Surface A, polished acrylic, $R_a = 3 \text{ nm}$, (b) Surface B, roughened acrylic ($R_a = 300 \mu\text{m}$), and (c) the *Ae. aegypti* tarsus. The bar plot in (d) shows takeoff preference by percentage of unfed *Ae. aegypti* from smooth (Surface A) and roughened (Surface B) takeoff platforms. Genders, combined for this plot, are not statistically different.

Table 1. Takeoff measurements for push and leg-strike takeoffs ($N = 10$).

	m_{leg}	m_{body}	$U (\text{m s}^{-1})$	$U_L (\text{m s}^{-1})$	$\tau_{\text{bw}} (\text{m s}^{-1})$	$\tau_t (\text{m s}^{-1})$
Push	$33.1 \mu\text{g}$	2.06 mg	0.38 ± 0.17		5.5 ± 2.2	11.6 ± 1.6
Legstrike			0.35 ± 0.17	0.59 ± 0.06	9.6 ± 1.6	13.1 ± 2.3

The curves for F_{LS} and $F_{\text{P},\text{LS}}$ are given in figure 6(a) for a range of U_{leg} values. The upper bound of U_{leg} is set such that the striking leg does not exceed the mechanosensory threshold of 0.07 mN. Slower U_{leg} values require greater forces by the pushing legs. This model, however, will not predict the value of F_{P} given by equation (1) as $U_{\text{leg}} \rightarrow 0$ because a very slow U_{leg} will require very large pushing forces for a takeoff constrained to τ_w . Therefore, we must apply a lower bound $U_{\text{leg}, \min} = g\tau_i(m/m_{\text{leg}}) = 0.49 \text{ m s}^{-1}$, the minimum speed required to generate a force equal

to the mosquito weight, 0.02 mN. Below $U_{\text{leg}, \min}$ the striking leg cannot generate upward motion.

By choosing the intersection of the curves in figure 6(a), $U_{\text{leg}} = 0.64 \text{ m s}^{-1}$ and $F_{\text{P},\text{LS}} = 0.027 \text{ mN}$, a model mosquito minimizes the greatest force exerted on the host substrate, minimizing the chance of detection. We note the force-minimizing leg-strike velocity predicted by our model is very close to the observed average of 0.59 m s^{-1} .

The curves for power produced by a striking leg, P_{LS} , and pushing leg, P_{P} from equations (2) and (4)

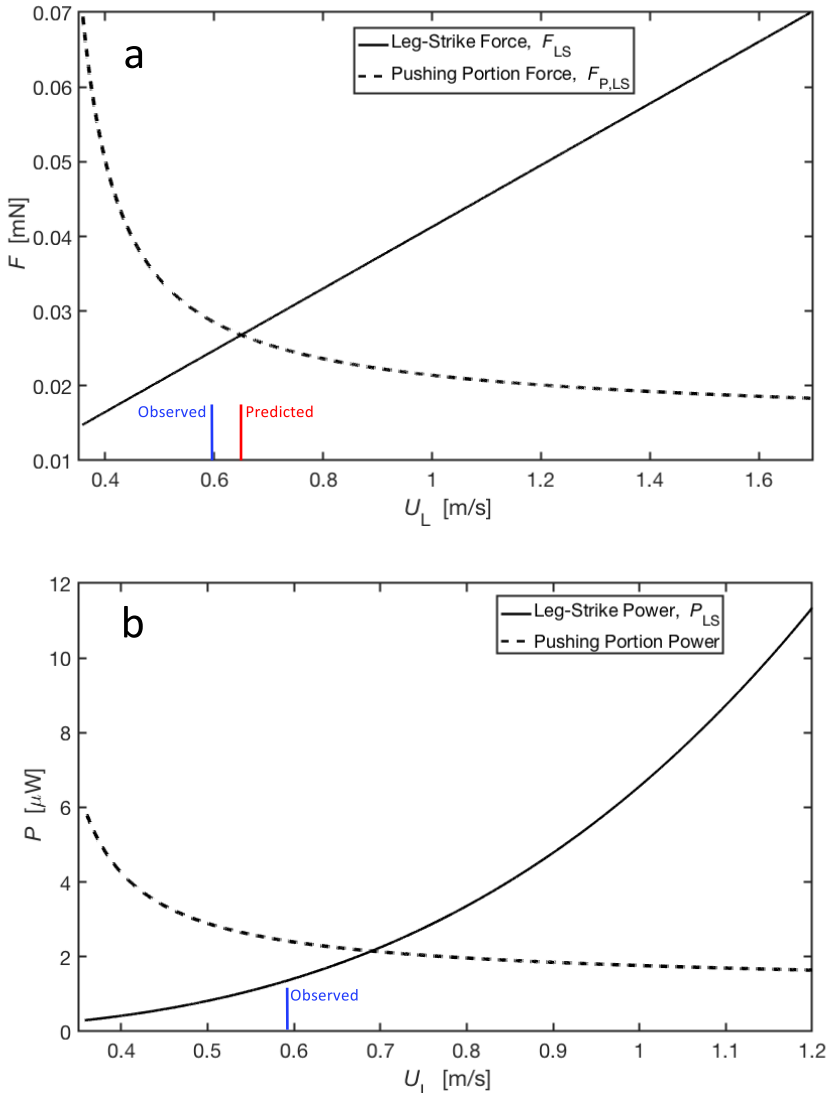


Figure 6. Model generated plots show the variance of leg-strike and pushing (a) forces and (b) power across a range of leg-strike impact velocity. The model predicted impact velocity based on force of 0.65 m s^{-1} is close to the observed average of 0.59 m s^{-1} .

respectively, are shown in figure 6(b). We note the intersection of these curves lies at $U_{\text{leg}} = 0.69 \text{ m s}^{-1}$ and $2.16 \mu\text{W}$, less than half the pushing power of a leg in a purely push takeoff at $5.78 \mu\text{W}$ (section 3.1). According to our model, at the observed leg-strike velocity of 0.59 m s^{-1} , the force and power of a pushing leg following the leg strike is 0.029 mN and $2.4 \mu\text{W}$. We therefore conclude the choice of U_{leg} is driven by reaction forces and not leg power.

4. Discussion

Our study reveals that *Ae. aegypti* mosquitoes employ two distinct takeoff strategies, a push and a leg-strike, and each strategy's proportion of utilization is influenced by takeoff surface roughness. To combat tarsal slipping on smooth surfaces, a leg-strike provides an initial boost skyward, decreasing the effort required by the subsequent pushing phase. Leg-strokes also consume 75% more time to execute than a purely push-based takeoff, while still producing a nearly

identical vertical velocity of $\sim 0.35 \text{ m s}^{-1}$ at the instant of first full wingbeat. The extra time is consumed by swinging a hind leg downward, producing a force comparable to the force of a pushing leg.

A greater understanding of the leg dynamics in launching mosquitoes may lead to enhanced functionality of uAS and terrestrial robots alike. Robotic jumpers [29–35] utilize the ubiquitous biological strategy of jumping to locomote across challenging terrain [34–36], a technique likely to be utilized in the next generation of extraterrestrial explorers [37–39]. Jumping permits flyers to become airborne before engagement of in-flight thrust sources, while terrestrial jumpers gain the ability to navigate difficult terrain not suitable for more common wheel- and track-based travel. Challenges robotic jumpers must overcome include takeoff angle modulation, self-righting upon landing, sequential jumping, and steering. Certain robots, such as the ‘sand flea’ [40], are able to jump tens of feet. However, certain terrain stands to challenge the robots’ design, which results in the inability to achieve

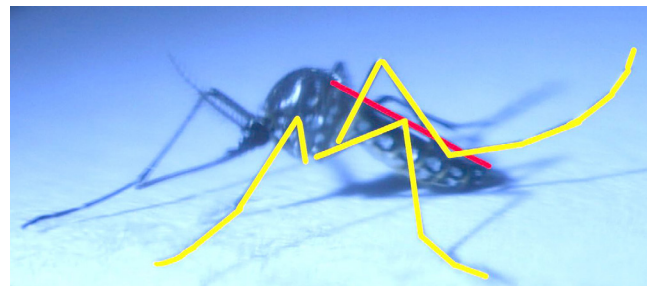


Figure 7. Photo of a resting mosquito with wings traced in red and left legs traced in yellow, showing the obstruction of wing traversal to the flapping plane by the legs.

maximum height, distance, and steering [29]. In the case of a polished surface such as ice, the performance of jumpers may be compromised, particularly those which rely on pushing appendages which contact the ground away from the center of mass. However, the utilization of a mosquito-inspired two-stage jump may subvert or reduce detrimental slippage. Such takeoffs may allow biomimetic devices an enhanced ability to optimize launch behaviors within power and speed limitations while encountering a myriad of terrain features.

4.1. Determination of pushing force and power

For takeoffs which employ as few as four pushing legs, the figures for force and power presented above must be recalculated. For purely pushing takeoffs, $F_p = 0.041$ mN. For leg-strike takeoffs, the pushing phase legs would exert $F_p = 0.043$ mN. We note these values remain well below 0.07 mN limit [21], which suggests the choice in number of participating legs is more critical for takeoff stability or direction than takeoff performance.

The assumption of constant F_p over the entire course of pushing motion provides an average value. If this assumption is violated, the average force value can be much less than the peak value. We may alternatively find F_p over the time course of takeoff by examining upward motion of the mosquito body and assuming the body is rigid and not rotating. Second order numerical differentiation of the thorax track in figure 3 produces a temporal curve for F_p given in figure S2, corresponding to an upward body acceleration of 11.3 gravities (g). The peak force per leg is 0.038 mN, with an average of 0.030 mN over 5.2 ms. We note this peak force is less than 0.07 mN and not dramatically greater than the previously calculated $F_p = 0.027$ mN. If only four legs are engaged in pushing, the peak push force would be 0.058 mN per leg.

In comparison to fleas [41, 42] and leafhopper insects [23, 43], mosquitoes are not adept jumpers. Fleas (*Boreus hyemalis*) and leafhoppers (*Ulopa reticulata*) generate accelerations as high as 150 g and 235 g, respectively, by elastic recoil of a resilin spring within the thorax [23, 41]. In leafhoppers, the corresponding power per muscle mass for the hind leg extensors is 25 mW mg⁻¹, where muscle mass is taken to be 11% of

the body mass [23]. At just 11.3 g and using all six legs, it is unlikely mosquitoes employ elastic energy release when pushing, but instead use direct muscle contraction as in flight [44]. The mass of the mosquito's extensor muscles is unknown to the authors, but if we conservatively assume the combined extensor muscle mass for all six legs is 5% of the body mass, the mosquito would have a power per muscle mass value of 0.34 mW mg⁻¹, which is comparable to the power density of the in-flight muscles of other insects [44].

4.2. Determination of leg-strike force

During leg impact, the leg converts its kinetic energy into body lift over a sub-millisecond impact time. Predictions of leg-strike velocity given by our impact model in section 3.4 is sensitive to the magnitude of leg impact time. An increase in the impact time of 1 ms requires a doubling of the velocity of the striking leg. Fortunately for mosquitoes, this impact time is passively governed by the material properties of their leg segments and joints. Leg deformation upon impact sets the impact time. Mosquitoes possess tubular legs [10], enabling the legs to attain stiffnesses higher than solid legs of the same mass. Greater leg stiffness shortens impact times and according to equation (3) enables more efficacious force transfer. Clever choice of leg materials and geometry in biomimetic devices will enable optimal takeoff performance by controlling leg deformation.

4.3. Prediction of slipping losses

As tarsi slip on Surface A, a bit of takeoff energy from pushing legs is lost to friction during lateral motion. If we assume the mosquito generates the same force on Surfaces A and B, we may estimate the pre-leg energy lost to friction as $E_{\text{slip}} \approx F_p d_{\text{slip}} = 0.054 \mu\text{J}$, where $d_{\text{slip}} = 0.6 \pm 0.4$ mm, $N = 5$, is the distance of tarsal slip and F_d is estimated from equation (1). The per-leg energy used during a slip-free takeoff can be estimated as $E_p = F_p \Delta z = 0.036 \mu\text{J}$, where $\Delta z \approx 1$ mm is the change in height of the center of mass from a resting position to the first wingbeat. We note this approximation for pushing energy is in agreement with $\tau_w P_p = 0.025 \mu\text{J}$ from equation (2). Therefore a mosquito is poised to use $E_{\text{slip}} = (d_{\text{slip}}/\Delta z) E_p = 1.5 E_p$ for failure to choose the appropriate takeoff technique.

Leg-strike takeoffs reduce the energy lost to slipping by positioning the legs closer to an orthogonal posture with the surface prior to the pushing phase of takeoff and subsequently reducing d_{slip} to <1 mm.

4.4. Biological implications

As presented in section 3.3, there is no statistical difference between female and male utilization of takeoff procedure, implying the disparity in weight between the genders does not greatly impact takeoff preference. Furthermore, mosquitoes (*Anopheles coluzzi*) are able to modulate takeoff kinematics following a blood meal, in which their mass grows by $3\times$, to maintain their liftoff speed [6]. Blood-fed *Anopheles coluzzi*, weighing 80% more than the females we study, liftoff at 0.23 m s^{-1} . This suggests there may be an optimal vertical takeoff velocity envelope for insects at the scale of mosquitoes, or with similar wingbeat kinematics, but this remains an area for future research. If the *Ae. aegypti* used in this study were allowed to blood-feed, we likewise expect wings to assume a greater role in takeoff force generation and vertical velocities at first wingbeat to decrease.

While our study highlights the mechanics of leg-initiated takeoffs by mosquitoes, it does not answer why takeoffs begin with leg motion. We surmise that leg-initiated takeoffs performed by mosquitoes are not principally done for efficiency nor speed. Any energy savings gained by reducing the number of wingbeats, $O(10)$, performed is minute by comparison to the number of wingbeats performed over a single flight, $O(10^4)$. Wings, and membrane wings in particular, are known to have increased performance near the ground [45] due to vortex interaction with a solid surface. The unique wing stroke kinematics of mosquitoes [46] may induce instabilities near the ground, but this is unknown. Time savings from using legs are likely meager as well. The time of leg action prior to the first full wingbeat is less than 10 ms. If leg action were to achieve the same dynamical consequences of 5 wingbeats, a mosquito beating its wings at $608 \pm 41 \text{ Hz}$, $N = 3$, would consume 8.2 ms to achieve a comparable elevation. Therefore, the most likely cause for leg engagement is wing obstruction. As seen in figure 7 and Movies S1–S3, wings moving from their resting position to their flight posture need to traverse a plane that intersects resting legs. By rapidly extending the legs downward, the legs leave the region occupied by beating wings. In Movie S4, we provide an instance where a mosquito is able to flap into the spaces between the middle and hind legs during leg extension, with wings contacting legs during this action. It is not clear if such a strategy would be effective if legs remained completely static, but is clear that legs are extended prior to the first full wingbeat. In flight, outwardly extended legs are positioned forward and aft of the stroke plane.

Mosquitoes engaging a leg-strike sacrifice time for a low-slip takeoff, similar to *Drosophila* trading stability for acceleration in escape takeoffs [7, 19]. The shift

of takeoff strategy from one surface to another suggests that insects are capable of judging the suitability of surface for takeoff, a capability which likely extends to other families of insects. Examples of fine adjustments to takeoffs may include locust jumps from very loose sand or mosquitoes from liquid surfaces [28]. As takeoff surfaces become more complex, with surface features on the mesoscale, undiscovered takeoff techniques may emerge. Future studies are needed to explore the methods and limits of insect evaluation of surface characteristics from temporal and topographical perspectives.

5. Conclusion

In this study we find *Ae. aegypti* mosquitoes taking off from horizontal surfaces employ two distinct strategies of takeoff, a ‘push’ and a ‘leg-strike’, the choice of which is influenced by surface roughness. Both strategies produce similar upward body velocities as the insect begins to beat its wings, 0.38 m s^{-1} and 0.35 m s^{-1} respectively, and brief times, 5.5 ms and 9.6 ms. On the smoother surface tested, the majority of individuals (66%) employ a leg-strike action prior to a pushing action, which reduces tarsal slip. On the rougher surface, leg-strike frequency reduces to 44%. The push takeoffs have one phase prior to wingbeat commencement, the extension of the legs and the force exerted on the takeoff surface by each pushing leg remains below the mechanosensory threshold of human skin, 0.07 mN. By comparison, leg-strike takeoffs have three phases, the downward swing of a rear leg, the impact of the leg, and the subsequent extension of all legs. The forces exerted by the striking leg, 0.025 mN, and pushing legs, 0.027 mN, likewise remain below the aforementioned threshold. By fixing takeoff time and upward body velocity before the first full wingbeat, we conclude that mosquitoes choose a leg-strike velocity that allows them to minimize the peak force exerted to the takeoff substrate, potentially a human host.

Acknowledgments

We thank Dr Bradley J Willenberg, Alicia Willenberg, and staff for graciously supplying mosquitoes and the University of Central Florida for funding this research.

ORCID iDs

Nicholas M Smith  <https://orcid.org/0000-0003-2507-0358>

Andrew K Dickerson  <https://orcid.org/0000-0003-1220-1048>

References

- [1] Bode-Oke A T, Zeygami S and Dong H 2017 Aerodynamics and flow features of a damselfly in takeoff flight *Bioinspir. Biomim.* **12** 056006

- [2] Chen M W, Zhang Y L and Sun M 2013 Wing and body motion and aerodynamic and leg forces during take-off in droneflies *J. R. Soc. Interface* **10** 20130808
- [3] Sunada S, Kawachi K, Watanabe I and Azuma A 1993 Performance of a butterfly in take-off flight *J. Exp. Biol.* **183** 249–77
- [4] Ellington C 1980 Wing mechanics and take-off preparation of thrips (thysanoptera) *J. Exp. Biol.* **85** 129–36
- [5] Pond C M 1972 The initiation of flight in unrestrained locusts *Schistocerca gregaria* *J. Comparative Physiol. A* **80** 163–78
- [6] Muijres F, Chang S, van Veen W, Spitsen J, Biemans B, Koehl M and Dudley R 2017 Escaping blood-fed malaria mosquitoes minimize tactile detection without compromising on take-off speed *J. Exp. Biol.* **220** 3751–62
- [7] Trimarchi J and Schneiderman A 1995 Initiation of flight in the unrestrained fly *Drosophila melanogaster* *J. Zool.* **235** 211–22
- [8] Wood R J 2008 The first takeoff of a biologically inspired at-scale robotic insect *IEEE Trans. Robot.* **24** 341–7
- [9] Brooks R A and Flynn A M 1989 Fast, cheap and out of control *Technical Report* Massachusetts Inst of Tech Cambridge Artificial Intelligence Lab
- [10] Christophers S 1960 *Aedes aegypti (L.) The Yellow Fever Mosquito: its Life History, Bionomics and Structure* (Cambridge: Cambridge University Press)
- [11] Mountcastle A M and Combes S A 2013 Wing flexibility enhances load-lifting capacity in bumblebees *Proc. R. Soc. B* **280** 20130531
- [12] Dudley R 1995 Extraordinary flight performance of orchid bees (*Apidae: Euglossini*) hovering in heliox (80% He/20% O₂) *J. Exp. Biol.* **198** 1065–70
- [13] Ristroph L, Bergou A, Ristroph G, Coumes K, Berman G, Guckenheimer J, Wang Z and Cohen I 2010 Discovering the flight autostabilizer of fruit flies by inducing aerial stumbles *Proc. Natl Acad. Sci.* **107** 4820–4
- [14] Dickerson A K, Shankles P G, Berry B E and Hu D L 2015 Fog and dense gas disrupt mosquito flight due to increased aerodynamic drag on halteres *J. Fluids Struct.* **55** 451–62
- [15] Dickerson A K and Hu D L 2014 Mosquitoes actively remove drops deposited by fog and dew *Integr. Comparative Biol.* **54** 1–6
- [16] Dickerson A, Shankles P, Madhavan N and Hu D 2012 Mosquitoes survive raindrop collisions by virtue of their low mass *Proc. Natl Acad. Sci.* **109** 9822–7
- [17] Dickerson A K, Liu X, Zhu T and Hu D L 2015 Fog spontaneously folds mosquito wings *Phys. Fluids* **27** 021901
- [18] Dickerson A K, Shankles P G and Hu D L 2014 Raindrops push and splash flying insects *Phys. Fluids* **26** 027104
- [19] Card G and Dickinson M 2008 Performance trade-offs in the flight initiation of drosophila *J. Exp. Biol.* **211** 341–53
- [20] Bimbard G, Kolomenskiy D, Bouteleux O, Casas J and Godoy-Diana R 2013 Force balance in the take-off of a pierid butterfly: relative importance and timing of leg impulsion and aerodynamic forces *J. Exp. Biol.*
- [21] Li L et al 2011 The functional organization of cutaneous low-threshold mechanosensory neurons *Cell* **147** 1615–27
- [22] Parry D and Brown R 1959 The jumping mechanism of salticid spiders *J. Exp. Biol.* **36** 654–64
- [23] Burrows M and Sutton G 2008 The effect of leg length on jumping performance of short- and long-legged leafhopper insects *J. Exp. Biol.* **211** 1317–25
- [24] Sutton G and Burrows M 2008 The mechanics of elevation control in locust jumping *J. Comparative Physiol. A* **194** 557–63
- [25] Sutton G and Burrows M 2010 The mechanics of azimuth control in jumping by froghopper insects *J. Exp. Biol.* **213** 1406–16
- [26] Suratwala T, Steele W, Feit M, Shen N, Dylla-Spears R, Wong L, Miller P, Desjardin R and Elhadji S 2016 Mechanism and simulation of removal rate and surface roughness during optical polishing of glasses *J. Am. Ceram. Soc.* **99** 1974–84
- [27] Tchvialeva L, Zeng H, Markhvida I, McLean D I, Lui H and Lee T K 2010 Skin roughness assessment *New Developments in Biomedical Engineering* (Rijeka: InTech)
- [28] Wu C, Kong X and Wu D 2007 Micronanostructures of the scales on a mosquito's legs and their role in weight support *Phys. Rev. E* **76** 017301
- [29] Zhang J, Song G, Li Y, Qiao G, Song A and Wang A 2013 A bio-inspired jumping robot: modeling, simulation, design, and experimental results *Mechatronics* **23** 1123–40
- [30] Zhao J, Xu J, Gao B, Xi N, Cintron F J, Mutka M W and Xiao L 2013 Msu jumper: a single-motor-actuated miniature steerable jumping robot *IEEE Trans. Robot.* **29** 602–14
- [31] Aoyama H, Himoto A, Fuchiwaki O, Misaki D and Sumrall T 2005 Micro hopping robot with IR sensor for disaster survivor detection *IEEE Int. Safety, Security and Rescue Robotics, Workshop* (IEEE) pp 189–94
- [32] Kovac M, Fuchs M, Guignard A, Zufferey J-C and Floreano D 2008 A miniature 7g jumping robot *IEEE Int. Conf. on Robotics and Automation* (IEEE) pp 373–8
- [33] Kikuchi F, Ota Y and Hirose S 2003 Basic performance experiments for jumping quadruped *Proc. IEEE/RSJ Int. Conf. on Intelligent Robots and Systems* vol 4 (IEEE) pp 3378–83
- [34] Tolley M T, Shepherd R F, Karpelson M, Bartlett N W, Galloway K C, Wehner M, Nunes R, Whitesides G M and Wood R J 2014 An untethered jumping soft robot *Proc. IEEE/RSJ Int. Conf. on Intelligent Robots and Systems* (IEEE) pp 561–6
- [35] Noh M, Kim S-W, An S, Koh J-S and Cho K-J 2012 Flea-inspired catapult mechanism for miniature jumping robots *IEEE Trans. Robot.* **28** 1007–18
- [36] Armour R, Paskins K, Bowyer A, Vincent J and Megill W 2007 Jumping robots: a biomimetic solution to locomotion across rough terrain *Bioinspir. Biomim.* **2** S65
- [37] Howe S D, O'Brien R C, Ambrosi R M, Gross B, Katalenich J, Sailer L, Webb J, McKay M, Bridges J C and Bannister N P 2011 The Mars hopper: an impulse-driven, long-range, long-lived mobile platform utilizing *in situ* martian resources *Proc. Inst. Mech. Eng. G* **225** 144–53
- [38] Yoshimitsu T, Kubota T, Nakatani I, Adachi T and Saito H 2003 Micro-hopping robot for asteroid exploration *Acta Astron.* **52** 441–6
- [39] Montminy S, Dupuis E and Champliaud H 2008 Mechanical design of a hopper robot for planetary exploration using sma as a unique source of power *Acta Astron.* **62** 438–52
- [40] Ackerman E 2012 Boston dynamics sand flea robot demonstrates astonishing jumping skills *IEEE Spectr. Robot. Blog* **2** 1
- [41] Sutton G P and Burrows M 2011 Biomechanics of jumping in the flea *J. Exp. Biol.* **214** 836–47
- [42] Bennet-Clark H and Lucey E 1967 The jump of the flea: a study of the energetics and a model of the mechanism *J. Exp. Biol.* **47** 59–76
- [43] Burrows M 2007 Anatomy of the hind legs and actions of their muscles during jumping in leafhopper insects *J. Exp. Biol.* **210** 3590–600
- [44] Josephson R 1993 Contraction dynamics and power output of skeletal muscle *Ann. Rev. Physiol.* **55** 527–46
- [45] Bleischwitz R, de Kat R and Ganapathisubramani B 2016 Aeromechanics of membrane and rigid wings in and out of ground-effect at moderate reynolds numbers *J. Fluids Struct.* **62** 318–31
- [46] Bompfrey R J, Nakata T, Phillips N and Walker S M 2017 Smart wing rotation and trailing-edge vortices enable high frequency mosquito flight *Nature* **544** 92–5